

Pupil location algorithm combining VFC Snake model with Grayscale Features

Peipei Lv^{1,a}, Zhiming Wang^{1,b}

¹ School of Computer & Communication Engineering, University of Science & Technology Beijing, Beijing 100083, China

^alpeipei@xs.ustb.edu.cn, ^bwangzhiming@ies.ustb.edu.cn

Keywords: VFC Snake model, least square fitting algorithm, pupil location, Grayscale Features.

Abstract. Pupil location is one of the key steps for iris location as pupil boundary corresponds to iris inner boundary. But uneven illumination affects the segmentation result heavily. The pupil region is the darkest part in most of the images, but it's not the only part. The proposed algorithm is based on the grayscale features and the prior that the pupil of humans is approximate circle. Firstly, the eye image binarization is achieved and the coarse positioning of the pupil region based on the grayscale features is obtained. Then, the outer boundary of the coarse positioning region is taken as the initial contour of the VFC snake model and iterates for a few times. Thirdly, a round curve is gained by using least squares circle fitting algorithm for the curve contour points, and serve as the new initial contour to iterative again. Finally, repeating the third step until the curve moved to the pupil edge. A large number of experiments demonstrate that proposed algorithm gives accurate result for most of the CASIA-Iris-Lamp images.

Introduction

Biometric authentication technologies, such as fingerprint recognition, face recognition and iris recognition, become more popular. While among them, iris recognition is the most accurate and stable one. Iris location is the first and vital section of the iris recognition. Pupil location is also the key step for its edge as the inner side of the iris location.

Many researches have been done multiply on the iris location algorithm, and some of them are widely acknowledged. Daugman proposed an algorithm using discrete 2D Gabor[1,2] and his iris recognition system has practical high-performance. Not long after, Wilders proposed a new algorithm combining edge detection with Hough transform[3], but this algorithm needs a high computation complexity. Wang used the least square fitting algorithm for iris location[5] and Ye puts fast iris location based on grayscale features of the pupil[6]. All these algorithms achieve good results when the eye images are with few noises. But when there are light sources during iris image acquisition, directly using these algorithms will not be able to get desired results.

The VFC(vector field convolution) Snake model proposed by Bing Li and Scott T. Acton is a kind of active contour model(known as snake model)[7]. We can obtain a closed contour on the pupil boundary. Compared to other snake models, this model not only reduces the computational cost but also has superior robustness to noise.

We focus on the iris database of CASIA-Iris-Lamp which is a child library of the CASIA-IrisV3 acquired by Chinese academy of sciences, and the bright spots generated by the light sources are useful if locating in the pupil. We get the rough location of the pupil based on the grayscale features, and achieve the precise location of the pupil combined the characteristics of pupil as a nearly circular with VFC Snake model.

Background

Parametric Snake Model. Parametric Snake Model or the active contour model is a closed curve combined by a certain number of control points which can move under the influence of the internal force and the external force until the energy functional would not change and the curve is on the edge

of our interest. The internal force is associated with the curve itself and ensures the continuity and smooth, while the external force is mainly derived from the image and makes the curve move to the boundary or other features within an image[8].

A traditional snake is parametrically represented as $v(s)=(x(s),y(s))$ $s \in [0,1]$, and the energy functional could be written like this:

$$E_{\text{snake}} = \int_0^1 (E_{\text{int}}(v(s)) + E_{\text{ext}}(v(s))) ds. \quad (1)$$

The internal force is unique represented as:

$$E_{\text{int}} = (\alpha(s) | v_s(s) |^2 + \beta(s) | v_{ss}(s) |^2) / 2. \quad (2)$$

While different snake model corresponds to different external force, the snake model energy functional became

$$E_{\text{snake}} = \int_0^1 ((\alpha(s) | v_s(s) |^2 + \beta(s) | v_{ss}(s) |^2) / 2 + E_{\text{ext}}(v(s))) ds. \quad (3)$$

A snake model should satisfy the following Euler equation:

$$\alpha v''(s) + \beta v''''(s) - \nabla E_{\text{ext}} = 0. \quad (4)$$

$$F_{\text{int}} = \alpha v''(s) + \beta v''''(s). \quad (5)$$

$$F_{\text{ext}} = -\nabla E_{\text{ext}}. \quad (6)$$

$$F_{\text{int}} + F_{\text{ext}} = 0. \quad (7)$$

F_{int} represents the internal force, and F_{ext} represents the external force. When the curve moves to the edge of the interest, when Eq.7 established, the curve stops moving.

VFC Snake Model. The vector field convolution (VFC) snake model was proposed as a class of edge-based static external forces to replace the traditional one. The novel external force is defined by convolving a vector field kernel with the edge map[7]. The vector field kernel is represented as $k(x,y)$,

$$k(x,y) = m(x,y)\mathbf{n}(x,y). \quad (8)$$

Where $m(x,y)$ is the magnitude of the vector at point (x,y) , and $\mathbf{n}(x,y)$ is the unit vector from point (x,y) to the kernel origin $(0,0)$.

The VFC external force is calculated by the formula

$$F_{\text{vfc}}(x,y) = [u_{\text{vfc}}(x,y), v_{\text{vfc}}(x,y)] = f(x,y) * k(x,y). \quad (9)$$

And ‘*’ represents the convolution symbol.

The new Euler equation is

$$\alpha v''(s) + \beta v''''(s) + F_{\text{vfc}}(x, y) = 0. \quad (10)$$

F_{int} represents the internal force, and F_{ext} represents the external force. When moving to the edge of interest, the curve stops moving.

Image Features. Generally, the pupil region has several characteristics.(1)The gray levels are lower than the surrounding regions.(2)The gray levels are mostly like to be the lowest in the

image.(3)The gray levels are nearly on the same level among the region.(4)the pupil is a circular approximately.

But for images collected in this library using an iris sensor with a lamp turned on, As we can see in Fig.1 which is some of the image from CASIA-Iris-Lamp image database which is the child of CASIA-IrisV3[13] , the lamp projects in the eyes and forms bright spots in the eye images. This would make the middle region looks brighter than the surroundings. In order to reduce the influence of iris texture, the bright spots projected by the lamp (BSL for short in this paper) have better in the pupil region, but we can't make sure of it. The only thing we are sure is that at least one BSL are in the pupil and their position relationship is determined.

There may be other regions as dark as the pupil region, and BSLs are always not the only brightest. But the BSLs in the pupil region can be easily found.



Fig.1. CASIA_Iris_Lamp image

Pupil Location

A flow chart has drawn to express our algorithm.

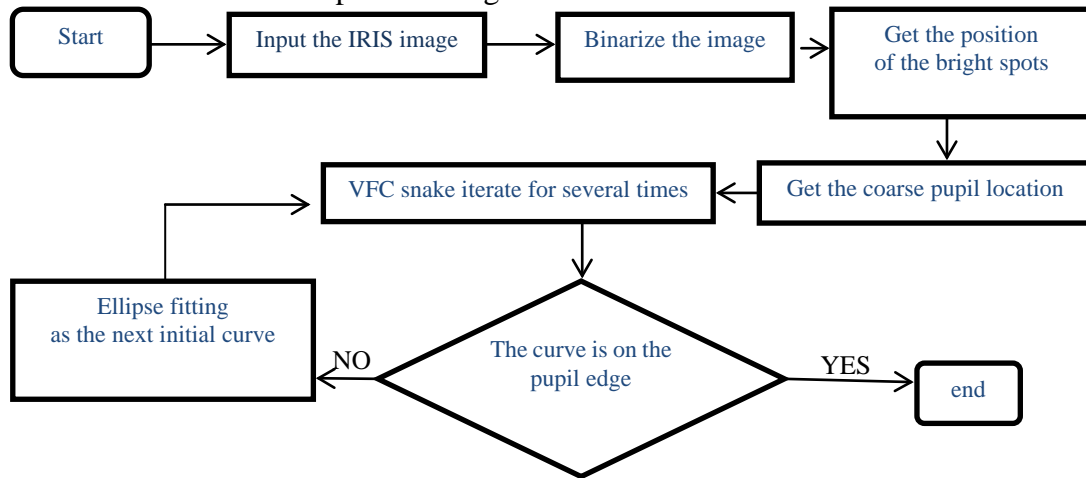


Fig.2. Flow chart of our algorithm

Image Binarization. The ideal binary image is the pupil region as foreground and other regions as background. But it's hard to be achieved.

Based on the prior knowledge that the pupil region has the lowest gray level, we introduce the minimum average gray value algorithm and divide every image into small regions with N pixels in width and N pixels in height. The image is scanned with the direction of row with every part as a unit, and the mean gray levels of every region were computed with the following formula

$$A_i = \frac{1}{N^2} \sum_{i=1}^N \sum_{j=1}^N I(x_i, y_j). \quad (11)$$

Meanwhile, all the mean gray levels along with their position were saved into a vector.

The following steps are finding out the regions with the smallest mean gray level or in a small range, and marking these regions on a new binary image, as shown in Fig.3.



Fig.3. Binary image

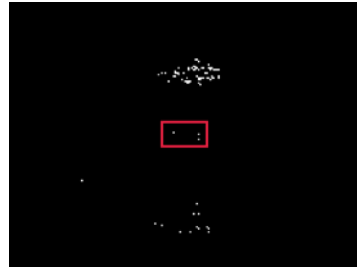


Fig.4. Bright spots

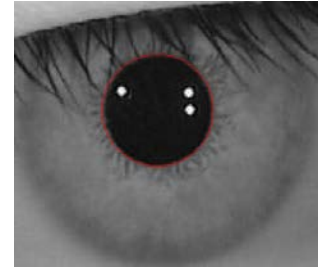


Fig.5. Coarse position with circular curve

Pupil's Coarse Location. Bright spots including the BSLs are always thought of noise, so previous papers would like to eliminate them directly. While bright spots have the highest gray levels which are 255 or close to 255, we can find them easily. If the ones in the pupil region were found, the pupil's location also can be confirmed. Scanning the original image to position all the bright spots, and estimating whether their surroundings were the foreground in the binary image to find the BSLs located in the pupil region. As shown in Fig.4, the three spots in the red rectangle is the BSLs, others are noise spots.

As the positions of the BSLs in the pupil are sought out, we can give the coarse location of the pupil. The steps can be described as follows, (a) Find the edge points of four directions and build a rectangle; (b) scan the binary image from the middle of the rectangle until the pupil edge and denote the left and right edges by X_{le} and X_{rg} ; (c) scan the vertical direction at $X=1/2(X_{le}+X_{rg})$, from the middle of the rectangle in vertical direction until the edge of the pupil, and denote the top and bottom edges by Y_{tp} and Y_{bt} ; (d) label the pupil region as circular, and calculate the center coordinates as well as the radius:

$$X_c=(X_{bt}+X_{tp})/2. \quad (12)$$

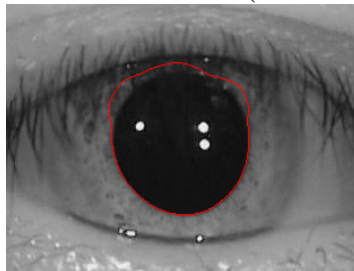
$$Y_c=(Y_{rg}+Y_{le})/2. \quad (13)$$

$$R=((X_{bt}-X_{tp})+(Y_{rg}-Y_{le}))/4. \quad (14)$$

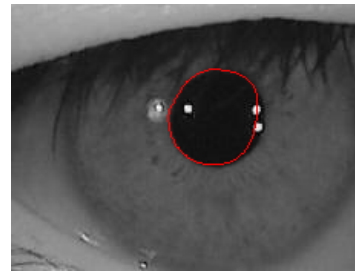
After these steps, as shown in Fig.4, a circular curve which is the coarse edge of the pupil has been obtained. What we can know from Fig.5 is that the coarse location of the pupil is correct basically, but not accurate.

Pupil's Accurate Location Based on VFC. Using the vector field convolution as the external force, we have to consider not only the vector field kernel but also the edge map. Edge map values have the character of being larger when closer to the edge of interest. For reason of keeping the edge information better, we choose the Canny edge as the edge map.

The circular curve generated in the section 3.2 is the initial curve of the VFC Snake model. But there are two exceptions. The first one is with the noise caused by the eyelashes or eyelid and the complexity of the texture distribution within the iris, if we use the VFC Snake model without any improvement, the snake curve could not move to the pupil edge (shown in Fig.6(a)). While the second one is that the BSLs may locate on the edge of the pupil, we could not obtain the real edge of the pupil with the original VFC snake model (shown in Fig.6(b)).



(a)



(b)

Fig.6. The results with original VFC Snake Model: (a) the first exception; (b) the second exception

In view of the above consequences, we need to do some improvements to make the algorithm

much better for these situations. The prior information that the pupil is a circular approximately can help to form the constraint to the snake curve, and by adopting the combination of the region extraction and circle fitting algorithm, the snake curve is able to cross some certain noises. Concrete expression of the algorithm: First the initial circular curve moves under the VFC external force; Then after a certain number of iterations, use the curve control points do the least square circle fitting and obtain a new circular curve as new initial curve for the next round VFC Snake model iteration, do the iteration of this step until the curve is the edge of the pupil.

Experimental Results

This experiment is carried out on the iris database collected by the Chinese academy of science called CASIA-Iris-Lamp. In this database, image can be divided into the following situations based on the position relationship between BSLs and pupils.

(1) When three BSLs are all in the pupil, the results are shown in Fig.7.

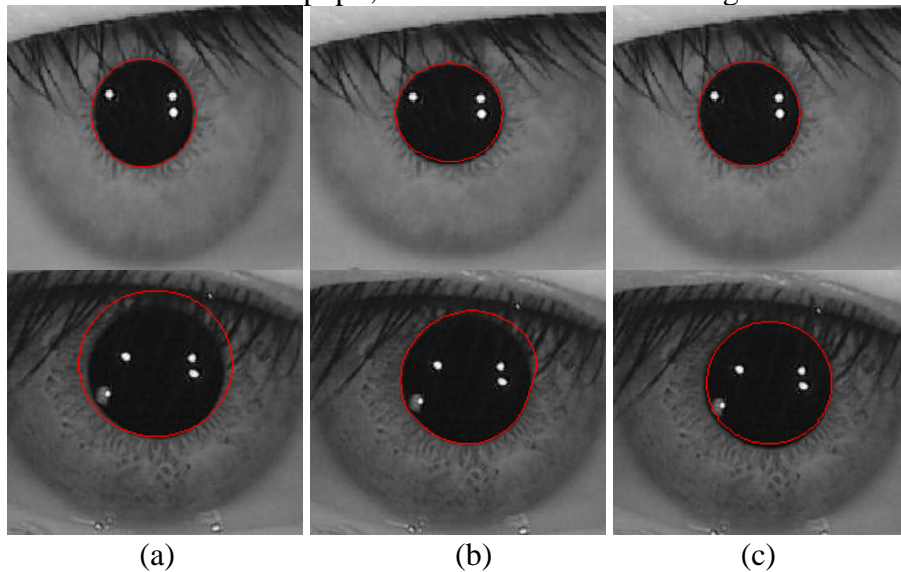


Fig.7. (a) the initial contours used our algorithm, (b) the results using traditional VFC snake model and (c) the results using our algorithm.

(2) When only one or two BSLs are located in the pupil, the results are shown in Fig.8.

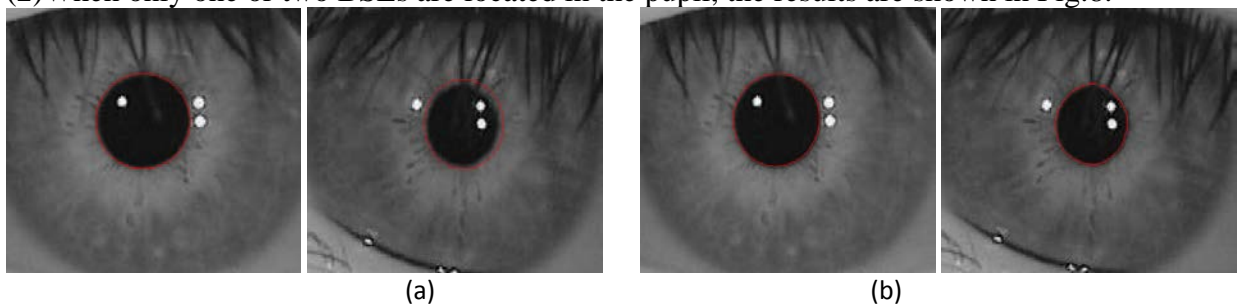


Fig.8. (a) the initial contour

(b) the results of our algorithm

(3) When some of the BSLs are on the edge of the pupil, the results are shown in Fig.9.

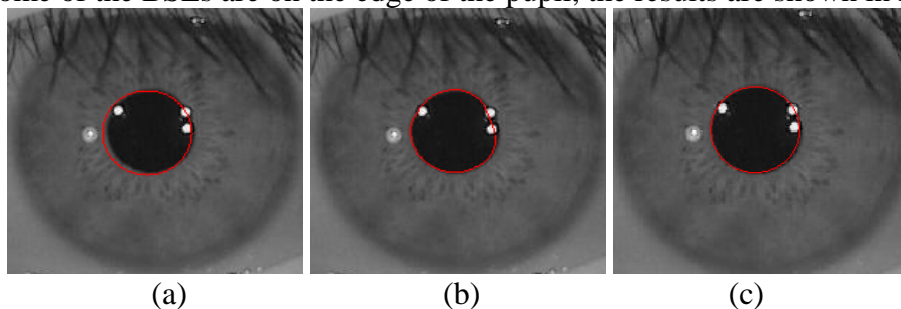


Fig.9. (a) the initial contours used our algorithm, (b) the results using traditional VFC snake model and (c) the results using our algorithm.

In this experiment, we compare our algorithm with the traditional VFC snake model with the same initial contour on every image and show the results.

From the figures above, we can see that this algorithm can get the correct boundaries for all these cases, while when there are noises such as eyelids and when the BSLs are on the edge of the pupils, the VFC Snake model without improvement can't get the correct edges. Our algorithm is more robust than the VFC Snake for this image database.

Conclusion

The proposed algorithm in this paper makes full use of prior knowledge about images in the database of CASIA-Iris-Lamp. We use the grayscale features about the pupil region and the BSLs as the basic of getting the coarse position of the pupil, and make its border curve as the initial curve of VFC Snake model achieving completely automation. Human pupil approximately round as a shape prior can help improve algorithm's noise resistance. Our algorithm can achieve the correct extraction of pupillary border without filling the bright spots. The accuracy of proposed algorithm lays a good foundation for the extraction of the outer boundary of IRIS. However our algorithm is unable to implement the correct segmentation of the pupil for cases such as the eyelids covering large pupil region, it will be improved our algorithm in our follow-up research.

References

- [1] J.G. Daugman. Complete discrete 2-D Gabor transforms by neural networks for image analysis and compression[J]. IEEE Transaction on Acoustics, Speech and Signal Processing. 1988, 36(7):1169-1179.
- [2] J.G. Daugman. High confidence personal identification by rapid video analysis of iris texture[J]. Proceeding of the IEEE, International Carnahan Conference on Security Technology, 1992:50-60.
- [3] Richard P.Wildes, Jane C.Asmuth, Gilbert L.Green, et al. A Machine-vision System for Iris Recognition[J]. 1996, 9:1-8.
- [4] Yuan Weiqi, Bai Xiaoguang. A new Iris Edge Extraction Algorithm[J]. Computer Vision Group, 2009, 29(8):2158-2164.
- [5] WANG YunHong, ZHU Yong, TAN TieNiu. Biometrics Personal Identification based on Iris Pattern[J]. National Laboratory of Pattern Recognition, 2002, 28(1): 1-10.
- [6] YE Yong-qiang, SHEN Jian-xin, ZHOU Xiao. Rapid Iris Location Algorithm Based on Grayscale Features of Pupil Regions[J]. Opto-Electronic Engineering, 2010, 37(3):127-132.
- [7] B. Li, T. Scott. Active contour external force using vector field convolution for image segmentation[J]. IEEE Transactions on Image Processing, 2007, 16(8):2096-2106.
- [8] M.Kass, A.Witkin. Snakes: active contour models[J]. International Journal of Computer Vision, 1987, 1(4):321-331.
- [9] I.Matveev, K.Gankin. Iris Segmentation System Based on Approximate Feature Detection with Subsequent Refinements[J]. International Conference on Pattern Recognition, 2014:1704-1709.
- [10] Ma Yide, Zhou Lijun, Li Yuan. Iris location algorithm by vector field convolution[J]. Infrared and Laser Engineering, 2014, 10: 3497-3503.
- [11] Information on <http://www.cbsr.ia.ac.cn>.